Journal of Power Sources 221 (2013) 356–365

Contents lists available at SciVerse ScienceDirect

Journal of Power Sources

journal homepage: www.elsevier.com/locate/jpowsour

Ageing and thermal conductivity of Porous Transport Layers used for PEM Fuel Cells

O.S. Burheim [c], G. Ellila [c], J.D. Fairweather [d], A. Labouriau [d], S. Kjelstrup [c], J.G. Pharoah [a,b,*]

[a] Queen's-RMC Fuel Cell Research Centre, 945 Princess St., 2nd floor, Kingston, ON, K7L 5L9, Canada
[b] Mechanical and Materials Engineering, Queen's University, Kingston, ON, K7L 3N6, Canada
[c] Department of Chemistry, Norwegian University of Science and Technology, 7491 Trondheim, Norway
[d] LosAlamos National Laboratory, P.O. Box 1663, MPA 11, MS D429, LosAlamos, NM 87545, United States

ARTICLE INFO

Article history:
Received 18 May 2012
Received in revised form
9 August 2012
Accepted 10 August 2012
Available online 21 August 2012

Keywords:
Polymer Electrolyte Fuel Cell (PEFC)
Through-plane thermal conductivity
Porous Transport Layers
Ageing
PTL
GDL

ABSTRACT

The through-plane thermal conductivity of artificially aged SGL Porous Transport Layers, PTLs, are measured and reported. NMR measurements of PTFE content and water/PTL contact angles are also reported. The PTLs were artificially aged in air rich water at 80 °C for 0, 200, 400, 600, 800, and 1000 h.

For the dry samples, it was found that the through-plane thermal conductivity did not change significantly in response to the ageing treatment. For the samples containing water, the through-plane thermal conductivity increased by a factor of two to three and the more aged samples had the highest thermal conductivities.

The through-plane thermal conductivity of dry PTLs is known to decrease with increasing PTFE content, which was also seen in this study. The chosen ageing procedure is known to wash PTFE from the PTL, and this verified using NMR. Water-PTL contact angle measurements also demonstrate that the PTL becomes less hydrophobic with ageing. This coincides with the increase in the through-plane thermal conductivity. Because the dry PTL retains its thermal conductivity while the PTFE content decreases we suggest that the PTFE remains in the fibre to fibre contact region and is removed predominantly elsewhere.

1. Introduction

The low temperature Polymer Electrolyte Fuel Cell, PEFC,[1] can convert the chemical free energy of the hydrogen oxygen reaction into electric work with high efficiency. For automotive applications, degradation (ageing), thermal management and cost reduction are important factors for commercial success. In this paper we discuss ageing processes for some PEMFC components with regards to thermal conductivity, Poly Tetra Fluor Ethylen (PTFE) loss and water management.

1.1. Ageing of PEM Fuel Cells

Durability is directly related to return on investment and thus ageing implications are important. Increasing lifetime while reducing the cost of the PEFC are considered by many to be equally important for the future success of large scale PEFC systems [1,2]. Accordingly, predicting ageing effects through accelerated ageing and stress tests are of great importance in PEFC development.

The traditional scope of ageing studies relates to the Membrane Electrolyte Assembly (MEA). Studies ranging from the order of 1000 h up to 26,000 h (equivalent to almost 3 years continuous operation) reveal that the PEMFC MEA can in fact retain its performance for as long as needed in automotive[2] applications even when exposed to hostile conditions [1,3].

Several studies have been undertaken to elucidate the phenomena affecting Porous Transport Layer (PTLs) and Micro Porous Layer (MPLs). Freeze cycles were investigated by Lee et al. [4], but found not to affect the mechanical properties of PTLs. Heat and humidity between 80 and 120 °C were found to adversely affect mechanical properties and to increase the water permeability. By studying the loss of PTFE from gas diffusion electrodes, where the X-ray Photon Spectroscopy (XPS) signal probed the electrode layer. Schulze et al. [5] found that ageing led to a loss in

* Corresponding author. Queen's-RMC Fuel Cell Research Centre, 945 Princess St., 2nd floor, Kingston, ON, K7L 5L9, Canada. Tel.: +1 613 533 6579; fax: +1 613 533 6489.
E-mail address: pharoah@me.queensu.ca (J.G. Pharoah).

[1] Sometimes referred to as Proton Exchange Membrane Fuel Cell (PEMFC).

[2] Automotive applications requires more dynamic tests than the continuous one of 26 000 h.

0378-7753/$ – see front matter © 2012 Elsevier B.V. All rights reserved.
http://dx.doi.org/10.1016/j.jpowsour.2012.08.027

PTFE content. According to Yuan et al. [2] the DOE has not developed a test procedure for this purpose and they explain that the PTL is the least studied material in terms of ageing. Recently, Kumar et al. [6] polarised both paper and cloth PTLs in 0.5 M sulphuric acid for 100 h at 80 °C and 1.2 V vs Saturated Calomel Electrode (SCE). They found that the paper type PTL oxidised less than the cloth, probably due to the degree of graphitization of the respective fibres.

While there is a lack of standard procedures for artificially ageing PTLs, it has been demonstrated that humidity and elevated temperatures affect the PTFE content and accordingly the hydrophilic properties. It is therefore expected that heating of PTLs for several hundred hours in oxygen rich water is a reasonable option for accelerated age effect testing. New means and standards for such *ex-situ* ageing procedures are however needed.

1.2. Heat and work of the PEFC

Despite the high efficiency of a PEFC there is always heat release associated with this process for at least three reasons [7–9]. The temperature multiplied by the change in the reaction entropy and the current divided by the Faraday constant, $T\Delta Sj/nF$ is a reversible and inevitable heat source in a PEMFC. The Tafel (or Butler–Volmer) equation predicts that increased current densities (reaction rates) necessarily result in additional losses, i.e. a reduction in the cell potential by an over-potential, η, with a corresponding heat release. This is the origin of the second heat source which is numerically the product of the current and the over-potential, ηj [10]. Finally, the Joule or ohmic heat is due to ohmic potential losses, R_Ωj, most significantly in the membrane, and is given by $R_\Omega j^2$. It is clear from the first law of thermodynamics that energy that is dissipated as heat is not available as work. The second and the third term represent irreversible processes (losses) whereas the first term is dictated by the sign of the entropy change for the reaction and is opposite in the reverse reaction. In the case of a PEMFC however all three terms represent heat generation and a corresponding reduction in available electric work from the fuel cell.

Heat generation in the fuel cell also necessarily results in temperature gradients within the cell which are dramatically impacted by the thermal properties of the cell materials. The Porous Transport Layer (PTL), sometimes referred to as the gas diffusion layer (GDL), is the thickest material and also the material sandwiching the main heat generation sections of the PEMFC and is hence the most important material for evaluation and engineering with respect to temperature gradients in the cell.[3] The PTL thermal conductivity is significant in setting the temperature at the electrode and hence its performance and its degradation rates. The temperature also changes significantly the water phase and rates of phase change which have a direct impact on both the cell performance and the degradation rates. The water phase change can in fact represent the largest heat source and/or sink in the fuel cell electrodes [12,13] and the state of the water present also strongly affects the heat handling of the PTLs.

Mathematical models of fuel cells accounting for temperature gradients have become more common over the last decade, as is well summarised by Bapat and Thynell [14]. Good predictions rely on good determinations of the thermal conductivity of fuel cell components. On the one hand one wishes to have the electrodes operating at a temperature as high as possible because this lowers – CO poisoning of the catalyst and improves the charge transfer kinetics (lowering η) [15]. On the other hand, it is desirable to increase material durability by keeping the membrane temperature well below the polymer glass transition temperature, T_g[4] [16,17]. Possible exposure to the glass transition temperature is dependent on both water content and temperature and constrains the upper limit for the operational electrode temperature. Since PEFCs are very often operated at a nominal temperature around 80 °C, a large temperature gradient in the PTL can result in membrane temperatures approaching T_g with a corresponding decreases in the membrane lifetime. Hence, knowledge of the PTL thermal conductivity both for virgin and aged materials is important in order to engineer a performant and durable PEFC. Large temperature gradients have also been shown to affect the cell water balance due to phase-change induced transport of water [18], further demonstrating that the fuel cell performance is dependent on the PTL thermal conductivity. Vie and Kjelstrup [11] used thermo-couples in the gas channels and between the electrodes and the membrane of a PEFC and measured more than a 5 °C temperature difference across the PTL, at a current density of 1 A cm^{-2}. Pharoah and Burheim [8] demonstrated, by the use of a mathematical model, that depending on the water phase change regime, gas flow channel design and the position in the electrode, the temperature differences between the gas channel and the electrode can be noticeably greater than 10 °C.

1.3. Thermal conductivity of PEFC components

Ex-situ measurement of the thermal conductivity of PTL materials is complicated for several reasons: *a*) the in-plane thermal conductivity has long been assumed [19–21] and recently experimentally shown [22–24] to be directionally dependent, *b*) the through-plane thermal conductivity, the thermal contact resistance and the thickness change with the applied compaction pressure [25,26], *c*) and residual water in the pores significantly changes both the thermal conductivity and the thermal contact resistance [25,26]. In measuring the thermal conductivity of PTLs care must be taken to properly account for the *in-situ* thickness, heat flux and temperature difference across the sample.

Several theoretical approaches have been made to calculate the thermal conductivities of PTL materials. By combining calculation and measurements, Ramousse et al. [27] estimated minimum and maximum thermal conductivities of carbon papers based on a previously developed model [20], connecting the thermal resistances of the solid and gas phases in parallel and in series, according to the Maxwell model. Sadeghi et al. [21] developed an analytical model to predict thermal conductivity from the material structure, simplified by assuming a basic repeating structure.

One important subject of discussion of thermal conductivity measurements has been the relation between thermal conductivity of the sample, the contact resistance between the sample and the apparatus and also the contact resistance between stacked samples [27]. Ramousse et al. stated that the contact resistance should be bounded by the resistance of layers of either air or carbon with the thickness of an individual PTL fibre. Our measurements of this contact resistance are approximately 2×10^{-4} m^2 K W^{-1} [25] which, assuming a fibre thickness of order 5 μm corresponds to a thermal conductivity of the order 0.025 W K^{-1} m^{-1}, which is the same as that of air. The challenge with a finite contact resistance between individual papers in a stack is that for every added sample

[3] This is verified experimentally [11] and by modelling [12]. This is because of several factors. The PTL is the thickest component in the PEMFC (after polarisation plates). It has the second lowest thermal conductivity (after Nafion). It insulates the heat production region in a PEMFC, i.e. the membrane electrolyte assembly (MEA).

[4] The T_g is the temperature at which a sudden reduction in mechanical strength of a polymer occurs. In the case of Nafion, the presence of water lowers this value from ~150 to ~100 °C depending on the presence and state of water next to the membrane material.

one also adds one more sample–sample contact resistance and hence, there are more unknowns than equations. By carefully sorting individual pieces of a PTL according to thickness, and comparing these results to the case of stacking multiple samples, Burheim et al. [25] were able to demonstrate that the sample–sample contact resistance is negligible. This result is physically satisfying as the contact between two individual samples is not dissimilar from the contacts between fibres within a single sample. We shall return to this discussion when discussing measurements of papers with Micro Porous Layers (MPLs) in Section 3.2.

The first *in-situ* experimental results for the through-plane thermal conductivity were reported by Vie et al. [11], giving a thermal conductivity of 0.19 ± 0.05 W K^{-1} m^{-1} for an ETEK ELAT PTL. The experiments were carried out by inserting thermocouples inside a fuel cell and results were obtained from a simplified thermal model. The relatively large thermocouples increased the uncertainty in the temperature gradient determination in these measurements. The first *ex-situ* experiments of thermal resistance were reported by Ihonen et al. [28], reporting the thermal impedance including both the bulk material resistance and the apparatus contact resistance of compressed PTLs (SIGRACET GDL 10-BC and Carbel CL). Khandelwal and Mench [29] reported the first *ex-situ* measurements of PTL materials with a perspective on de-convoluting the thermal conductivities and their contacts to the apparatus. However the *in-situ* thickness was not taken into consideration and this has a direct impact on the determination of thermal conductivity. Ramousse et al. [30] used a similar approach. Their apparatus applied copper plates at the end of each cylinder, sandwiching the investigated sample. Using this experimental set-up, different PTL materials provided by Toray (3 different thicknesses) and SIGRACET were tested by measuring the thermal resistance of stacks of samples. The first experimental report giving all of the three parameters required by Fourier's law as a function of compaction pressures was that of Burheim et al. [25]. Correcting for the actual thickness corrects the reported values by 5–20% depending on the PTL materials and the compaction pressure. More importantly was that we demonstrated that the PTL–PTL contact thermal resistance is negligible and that neglecting this when stacking materials is a valid approach when measuring through-plane thermal conductivity.

The impact on thermal conductivity introduced by changing the temperature both for in- and through-plane thermal conductivity was measured by Zamel et al. [24,31] For through-plane thermal conductivity with controlled compression; it was found that at 16% compression (unknown compaction pressure) the thermal conductivity of the PTL, regardless of PTFE content, does not depend significantly on temperature [31]. For the in-plane thermal conductivity it was found that for PTFE free PTLs the thermal conductivity is lowered by ~50% when comparing values measured at room temperature to values from measurements undertaken at 60 °C and higher [24]. For the PTFE treated samples, the in-plane thermal conductivity is nearly unaffected in the range of −20 to +120 °C, respectively [24]. This is similar to what Khandelwal reported for Nafion [29].

For the first time we study and report the ageing impact on the thermal conductivity of PTLs, not only as a property in itself, but also as a mean to understand the ageing mechanism of PTLs and the PTFE therein. This is of great importance when evaluating previous degradation studies and also for the design of new PEMFC materials.

2. Theory and experimental

2.1. Apparatus

The apparatus used in the experiments is depicted in Fig. 1 and is described in greater detail in Ref. [25]. The thermal

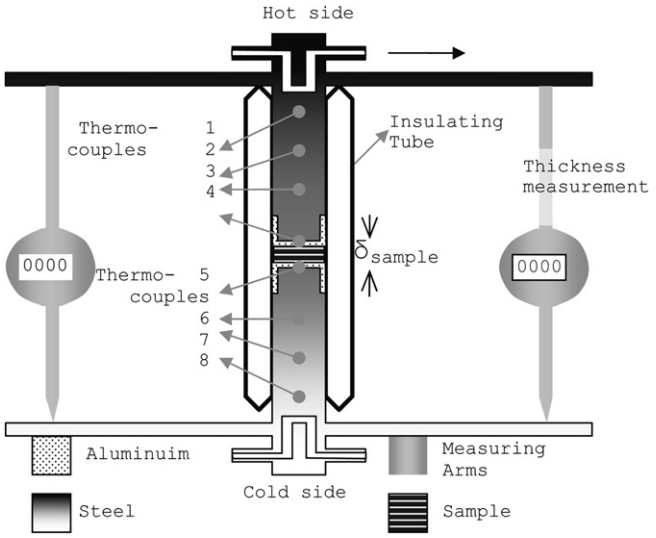

Fig. 1. A 2D sketch of the apparatus used to measure thermal conductivity as reported here [25,26].

conductivity apparatus was designed to simultaneously measure the variables that appear in the discrete form of Fourier's law, i.e. the heat fluxes q_i, the sample thickness, δ_s and the temperature drop over the sample. The heat flux is measured on each side of the sample along with the temperature drop over the sample and the thickness of the compressed sample material, as in Eqs. (1)–(3). In this context the term "sample" refers to a stack of materials and the contact to the apparatus. Next, the thermal resistance and its contact to the apparatus were plotted as function of the measured thickness in order to de-convolute the thermal conductivity and the thermal contact resistance. (See Eqs. (4) and (5) in Section 3.2.3.) The measurements were carried out at three different compaction pressures, 4.6 bar, 9.3 bar and 13.9 bar. These were applied pneumatically and read from the gas bottle regulator. The upper temperature was held at 35 °C while the lower temperature was maintained at 10 °C such that the sample temperature is very close to room temperature. Each sample was left for at least 10 min in order to reach a steady state and then temperature data was recorded at 30 s intervals for 10 min and averaged. Except in the case of samples with MPLs, which is described below, measurements are taken for stacks of 1, 3, and 5 samples (9 different samples in total) and the conductivity and contact resistance determined from a linear regression based upon these three measurements. q_i/[W m^{-2}], k_i/[W K^{-1} m^{-1}], T_i/[K], δ_{i-j} and R_i/[K m^2 W^{-1}] are the heat flux, thermal conductivity, temperature, length/thickness and thermal resistivity of region, position or material in agreement with Fig. 1, respectively. An example of a measurement, using SGL DA, is given in A.

$$q_{\text{upper}} = k_{\text{steel}}\frac{T_1 - T_3}{\delta_{1-3}} \tag{1}$$

$$q_{\text{lower}} = k_{\text{steel}}\frac{T_6 - T_8}{\delta_{6-8}} \tag{2}$$

$$q_{\text{sample}} = \frac{q_{\text{upper}} + q_{\text{lower}}}{2}, \quad \text{and;} \quad R_{\text{sample}} = \frac{T_4 - T_5}{q_{\text{sample}}} \tag{3}$$

2.2. Procedure

Several of the samples in the present study are coated with a MPL. In stacking these we consider a repeat unit to be a pair of samples with the MPL coated sides contacting. In this way, the sample to apparatus contact resistances are the same at each contact and should be the same as in the cases with no MPLs. In addition, the repeat unit to repeat unit contact resistance is also the same as in the case with no MPL and can reasonably be expected to be negligible, as discussed above. Finally, within each repeat unit there is one MPL–MPL contact which may or may not be negligible but which if present will be lumped into the conductivity. This approach, however, requires additional sample materials, which were in short supply. Accordingly, we measured A, one repeat unit (two MPL coated PTL discs), B two repeat units (four MPL coated PTL discs) and C, A and B stacked together for a total of three repeat units at the cost of having to re-use the samples. This was carried out first at the lowest compaction pressures (4.6 bar), next at the intermediate (9.3 bar) and lastly at the highest compaction pressure (13.9 bar). Thus possible hysteresis effects from high compaction pressures [32,33] were avoided. Before carrying out these experiments, several samples and sample stacks were measured multiple times by disassembling and reassembling in between these repeated measurements with no significant effect on the measured values. Thus we made sure that our A, B, C procedure was valid at a constant repeated compaction pressure.

2.3. Artificially ageing Porous Transport Layers

PTL samples were heated in deionized water for approximately 0, 200, 400, 600, 800 and 1000 h at 80 °C. This procedure was carried out in environmental chambers machined from PTFE, to minimize cross-contamination between the chamber walls and the samples. The water was constantly purged by bubbling air to more closely simulate the PEMFC cathode environment. Moreover, water vapour in the effluent air was condensed in a length of chilled Teflon tubing and refluxed to maintain the water level. The temperature in each chamber was held constant *y* a hot plate linked to a Teflon-coated thermocouple probing the water.

2.4. Incorporating water in the PTLs

For the PTLs not coated with MPLs, experiments were undertaken with water in the samples. The technique for achieving this is previously reported [25,26] and thus only briefly repeated here. As is depicted in Fig. 2, there is a small water reservoir above one or a stack of PTLs and water is forced through sample using an aspirator suction pump. The suction was gradually turned on until water started to flow through the sample. The water process was stopped before the reservoir was emptied. In total, less than one dl (100 cm^3) was fed during this step.

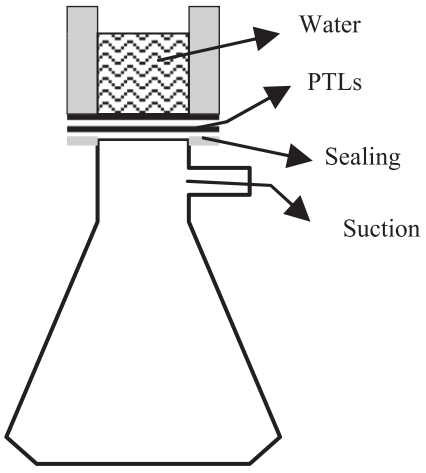

Fig. 2. Figure depicts the set-up for introducing water into the PTLs.

Water was fed first from one side and then next from the other side by flipping the stack and repeating the procedure. The amount of water retained by the sample, or the residual saturation, was determined by weighing the samples as follows; 1; the wet sample was cut to fit the rig, 2; the sample was weighed, 3; the sample thermal conductivity was measured, 4; the sample was dried, 5; the sample was weighed again.

Table 1
PTFE loading applied to the substrate as indicated by the first letter following the series number in the product specification.

First letter	A	B	C	D	E
PTFE-wt.%	0	5	10	20	30

2.5. Material selection

The chosen materials can be split into two groups, uncoated PTLs and MPL coated PTLs. The uncoated PTLs are more amenable to experiment and interpretation since they are intended to be homogeneous while the MPL coated PTLs are much closer to what is actually used in fuel cells but clearly have different properties in the substrate and in the MPL with an ill-defined interface between the two regions. While it is difficult to justify reporting a single thermal conductivity for such a composite systems, we have chosen to report 'conductivities' in order to be consistent with our previous work and the published literature. The conductivity numbers for materials with MPLs should however not be used in detailed models aimed at predicting temperature profiles within the materials though they can, of course, be safely used to predict the total temperature change across the material.

2.5.1. Sigracet PTLs

SGL Porous Transport Layers type 24 and 25 have been chosen for investigation in this paper. These are delivered with PTFE content in the range from 0 wt.% to 30 wt.%.[5] The specific papers used in this study are: SGL 24BC, SGL 24B"C", SGL 24DA, SGL24DC, SGL 24D"C" and SGL 25BC. The number 24 and 25 indicate the PTL product series, the first letter following this represents the substrate PTFE content (Table 1) and the second letter represents presence/composition of a MPL. The interpretation of first letter, the PTFE content, is indicated in Table 1 while an A for second letter indicates the absence of a MPL and any other letter represents the composition of the MPL as indicated in Table 2. This is illustrated in Fig. 3. The 25 series is more porous than the 24 series and also has a higher gas permeability as illustrated in Table 3.

2.6. Contact angle measurement

Since the thermal conductivity is strongly affected by the water content of a PTL, measurements of external water contact angle, α, were used to partially indicate changes to the hydrophobic

[5] This is not the weight percent of PTFE in the PTL, but the percentage of PTFE in the slurry forced through the material as a hydrophobic treatment. Subsequently after this treatment the PTL is dried and some of the PTFE remains in the material.

Table 2
PTFE loading of the MPL as indicated by the second letter following the series number in the product specification.

Second letter	A	"C"	C
MPL PTFE-wt.%	No MPL	5	23

Table 3
Selected properties of the substrates investigated in this study.

	Areal weight	Porosity	Air permeability
24BA	54 g m^{-2}	84%	60 $cm^3(cm^2s)^{-1}$
25BA	40 g m^{-2}	88%	210 $cm^3(cm^2s)^{-1}$

character of samples after ageing, see Fig. 4. The sessile drop method was used, applying five 1.0 μL droplets of water to each sample in a goniometer equipped with digital camera and analysis software. For each material 5 parallels were made.

2.7. Nuclear Magnetic Resonance – NMR

An important part of this study was to investigate possible PTFE degradation during ageing of PTLs. NMR allows to quantify the amount of PTFE in the bulk of the material. Most other composition analysis tools allows only for surface composition analysis. Hence, and due to availability, NMR was chosen for PTFE PTL bulk content determination.

19F MAS NMR spectra were obtained using a Bruker Avance 300 spectrometer operating at 282.4 MHz. The pulse length was 2.5 μs and 10 s delay time was used with a 4 mm fluorine free probe. A total number of 1024 scans were accumulated with a spinning rate of 11 kHz. Chemical shifts were referenced to external $CFCl_3$ at 0 ppm. Samples were prepared by mixing 12 mg of NaF, 25 mg of MgO and 50 mg of SGL 24DA.

2.8. Statistical analysis and accuracy of the measurements

The thermal apparatus was calibrated using materials with known thermal conductivity. These values are known with 5% accuracy and thus this level is the accuracy limitation of the reported values in this paper [25]. However, the thermal conductivities in the Results section reports deviations from the linear regression using a least square of residual approach. Due to the scarcity of samples, each of the regressions in this paper are based on only three points which means that a good linear fit is represented by a small error while a poor regression will have considerably larger error. All numbers are reported with 95% confidence intervals.

3. Results and discussion

A large variety of samples have been investigated in this study as listed above, and a selection of the most significant data is presented here. The thermal conductivity values are presented for those measurements undertaken at 9.3 bar compaction pressure, with values at different applied pressures tabulated in the Appendix. The sample series that are not taken into this report are left out because they provide no additional information, i.e. the trend with thermal conductivity as a function of artificial ageing time is as for the other materials and the thermal conductivity values are within in the window of the values for those tabulated in this paper. The vacancies in the tables, indicated by –, are due to a lack of material (in case of thermal conductivity) or selection by priority.

Fig. 3. Example sketch of PTL + MPL with different PTFE content.

3.1. Artificially aged PTLs

Table 4 gives the through-plane thermal conductivity, the thermal contact resistance to aluminium, the measurement sample thickness and (when present) the volumetric water saturation for SGL 24DA (dry), SGL 24DA (wet) and SGL 24BA (wet) as a function of artificial ageing time and the contact angle, α, between water and the dry PTL, respectively. The through-plane thermal conductivity and the thermal contact resistance data are also shown graphically in Fig. 5.

3.1.1. Dry PTLs

As discussed in the introduction, Section 1.1, heating the PTL materials in air purged water is expected to remove some of the PTFE and, as described in Section 1.3, this could lead to increased through-plane thermal conductivity. Examining the measured through-plane thermal conductivity of the dry SGL 24DA one can see that there are no significant changes induced by the chosen ageing procedure. This is also the result for the measured thermal contact resistance and the measured thickness. SGL 24DA is, in this study, the material with the largest PTFE content in the PTL base substrate and the absence of a change in the through-plane thermal conductivity was therefore surprising. NMR measurements indicate a significant change in the total content of PTFE before and after the ageing procedure, See Fig. 6. We shall return to this point in Section 3.1.2 and 3.3.

3.1.2. PTLs with liquid water

No significant changes were measured for the through-plane thermal conductivity for the dry PTL samples. For the samples containing water, we found an increase in the thermal conductivity and that this property increases with ageing time. Though the trend of increasing thermal conductivity with time is scattered, the water contact angle with the PTL substrate, α, decreases with ageing, while the liquid saturation, S, tends to increase. Furthermore, NMR spectroscopy, Fig. 6, shows that the SGL 24DA sample has lost a significant amount of PTFE by the end of 1001 h of ageing. All this indicates that the affinity of the samples for water is increasing with ageing, and this does indeed affect the thermal conductivity of the wet samples. This can be seen in Table 4 and in the graphical presentation to the left in Fig. 5.

Despite the large standard deviations in the reported values of the thermal conductivity it is beyond doubt that the value increases with the presence of water and also that this effect is stronger after

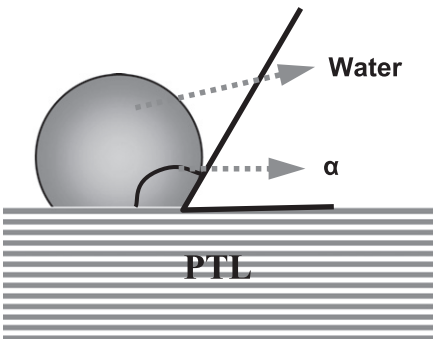

Fig. 4. Water droplet – PTL interface and contact angle, α.

Table 4
Overview of the measured thermal conductivity as function of ageing time for the selected materials at 9.3 bar compaction pressure. Units are; k_{PTL}/W K^{-1} m^{-2}, R_{Al-PTL}/10^{-4} K m^2 W^{-1} and δ_{PTL}/10^{-6} m, respectively. The water content, S, is defined as the fraction of the PTL pores filled with liquid water and is measured by weight before and after drying the samples. Also the contact angle, α, of water on the samples, in degrees, are given for some of the samples.

Time$_{aged}$	0 h	~200 h	~400 h	~600 h	~800 h	~1000 h
	SGL 24DA	Dry				
k	0.33 ± 0.02	0.31 ± 0.02	0.33 ± 0.01	0.32 ± 0.01	0.32 ± 0.01	0.33 ± 0.02
R_{Al-PTL}	1.2 ± 0.5	0.9 ± 0.5	1.1 ± 0.3	1.00 ± 0.17	1.12 ± 0.12	1.3 ± 0.6
δ_{PTL}	177 ± 16	188 ± 16	174 ± 12	175 ± 16	170 ± 5	167 ± 6
	SGL 24DA	Wet				
k_{PTL}	0.50 ± 0.14	0.585 ± 0.017	0.9 ± 0.3	0.6 ± 0.3	0.94 ± 0.04	0.9 ± 0.7
R_{Al-PTL}	1.7 ± 1.5	0.9 ± 0.1	2.5 ± 1.0	1 ± 2	3.38 ± 0.11	1.3 ± 1.7
δ_{PTL}	174 ± 5	170 ± 8	173 ± 12	168 ± 3	172 ± 9	175 ± 7
S	0.2 ± 0.2	0.2 ± 0.4	0.2 ± 0.4	0.3 ± 0.4	0.2 ± 0.3	0.4 ± 0.2
α	137 ± 5	–	129 ± 5	–	–	125 ± 5
	SGL 24BA	Wet				
k_{PTL}	0.39 ± 0.02	0.49 ± 0.018	0.6 ± 0.14	0.44 ± 0.06	0.49 ± 0.02	0.8 ± 0.5
R_{Al-PTL}	0.27 ± 0.01	1.3 ± 0.2	1.5 ± 1.1	0.8 ± 0.9	1.5 ± 0.1	2.7 ± 1.6
δ_{PTL}	171 ± 7	169 ± 6	167 ± 10	175 ± 17	165 ± 6	173 ± 5
S	0.1 ± 0.3	0.2 ± 0.3	0.2 ± 0.3	0.1 ± 0.1	0.2 ± 0.2	0.2 ± 0.2
α	135 ± 5	–	135 ± 5	–	–	124 ± 5

1000 h of ageing compared to the virgin material. The linearity of the trend with artificial ageing time is speculative in light of the current data. For this reason we have chosen to illustrate two possible trend lines for the thermal conductivity of SGL 24DA containing residual water. Looking also at the water content, S, one can see that it is hard to argue a significant difference between the two sets of data, i.e. SGL24 BA and DA. However there appears to be a weak trend for the water content, S, and the through-plane thermal conductivity to increase and for the contact angle and the PTFE content to decrease as a function of ageing time for the two set of samples. However whether this is related to some threshold change around 300 h of ageing (as indicated by the dashed step line) or if it is a continuous gradual material modification (As indicated by the straight ascending dashed line) can not definitively ascertained in this study. What is important is that all four measurements are consistent.

Water contact angles measured by the sessile drop method indicate that the PTL samples have become significantly less hydrophobic by 1000 h of ageing time. From Tables 4 and 5 one can see that the contact angle of the PTL is significantly changed while the contact angle of the MPL is not. This is consistent with the drop in PTFE content shown in Fig. 6. A previous study has suggested that this surface change is in part due to oxidation of the carbon surface, since the contact angle decrease is larger as the ageing environment is made more oxidizing [34]. Since less hydrophobic pores should be more easily filled with water, we expect that using the same water incorporation procedure should result in higher saturation of the aged samples. Moreover, these observations coincide with the NMR results of Fig. 6, in that less PTFE in the bulk substrate should allow a higher water saturation level, S.

From our experience [26], introducing liquid water to PTLs previously subject to a PTFE hydrophobic treatment gives far from reproducible results both regarding the water content, S, and the through-plane thermal conductivity, k. However, we do know that the thermal conductivity goes up by a factor ~2.5 for SGL 10AA and a factor 2–4 for Toray (0–5% wet proof) PTLs when water is introduced [26]. Also, even when the PTFE content is higher and the relative errors increase, the thermal conductivity increases when water is introduced to the hydrophobic treated PTLs [26].

Again we look to the dashed regression line and the values for the wet PTL shown in the left graph of Fig. 5. On the one hand, from the literature we expect more water and hence increased thermal conductivity with ageing, while, on the other hand, it is difficult to justify significance by statistical arguments for the present results. Moreover, the trend of increased thermal conductivity with ageing when water is present appears stronger for the SGL 24DA than for the BA, though, again, this is far from significant based on the measured values. All around, when comparing the wet to the dry PTL thermal conductivity; the thermal conductivity of the wet, non-aged PTLs are approximately twice as large as in the case of dry PTLs and threefold for those aged the longest. In the light of the reported contact angles, the water content and the NMR, the increase in thermal conductivity of the PTL with residual water is a reasonable and consistent set of results.

The increase in thermal conductivity, of a factor increasing from approximately two to approximately three, is very similar to what

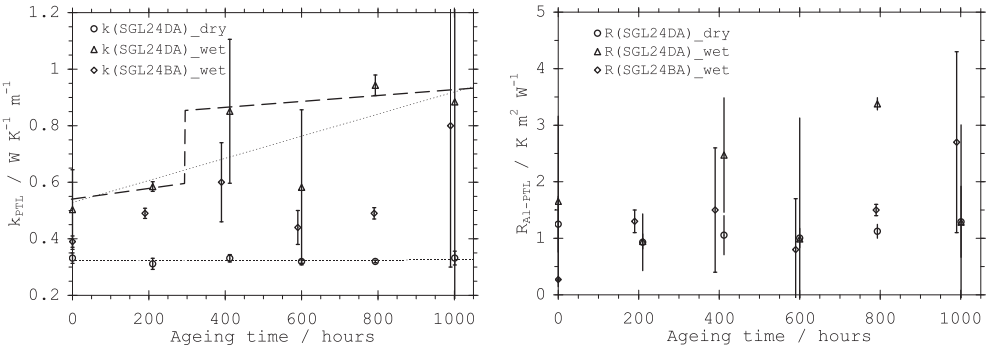

Fig. 5. Through-plane thermal conductivity (left) and thermal contact resistance to aluminium of SGL PTLs as function of artificial ageing time.

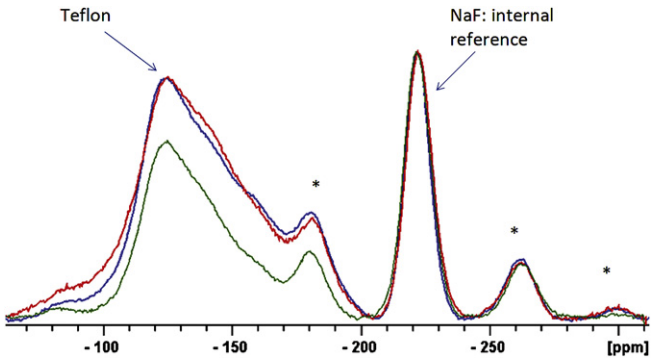

Fig. 6. NMR spectra of SGL 24DA using NaF as an internal reference; pristine (blue), 412 h aged (red) and 1001 h aged (green). (For interpretation of the references to colour in this figure legend, the reader is referred to the web version of this article.)

was seen for the SGL 10AA. This suggests that the contribution to the increase in thermal conductivity by the water is the same as what was seen and proposed in Ref. [25,26]. In these studies it was argued that water aids the heat conduction locally by enhancing the fibre to fibre contact regions rather than conducting heat via a bridge through the PTL material. This argument stems from the fact that the relative increase in thermal conductivity is far greater than that expected from the addition of a small volume fraction water as a heat-conducting phases in the pores. We shall return to this discussion in Section 3.3.

3.2. MPL coated PTLs

3.2.1. PTL PTFE content and MPL

In Table 5 we give the thermal conductivity and the measured thickness for the SGL 24DA, 24DC and the 24BC at 9.3 bar compaction pressure. The SGL 24DA and the 24DC differ by the addition of a MPL and the 24BC and 24DC have different PTFE contents in the PTL substrate.

Comparing the results for the SGL 24DA and 24DC, it is evident that introducing the MPL has little effect on the thermal conductivity. Previous estimates indicated a thermal conductivity of a MPL to be 0.5 ± 0.5 W K^{-1} m^{-1} at 9.3 bar compaction pressure [25] and therefore one might expect some increase in the overall thermal conductivity with the addition of a MPL. This is however not the case in the results of Table 5. In other words; the MPL hardly contributes to a change in the overall thermal conductivity while PTFE in the PTL substrate contributes to a decreased overall thermal conductivity. We therefore conclude that the initial PTFE content is more important to the PTL overall thermal conductivity than is the addition of a MPL.

Comparing the SGL 24BC to the 24 DC, it is apparent that the thermal conductivity of the 24DC is lower than that of the 24BC. This coincides with what is reported previously, that introducing PTFE in the PTL substrate decreases the thermal conductivity of the material [25,26,29]. What is important to note is that the PTFE content in the PTL substrate layer appears to impact the overall through-plane thermal conductivity much more than does the MPL. Moreover, it is worth noting that this effect does not change significantly with the ageing time. We return to this point in Section 3.3.

3.2.2. PTL porosity

One of the material pairs which appear similar but actually feature the largest difference in thermal conductivity is SGL 24BC and the SGL 25BC. These two materials are very similar with respect to PTFE content and MPL coatings. The difference between them is that the 25 substrate is reported by SGL to have lower areal weight and better gas transport properties than the 24 substrate (Table 3). This could for instance be due to the amount of binder in the PTL substrate. SGL 24BC is slightly less porous and, as can be seen from Table 6, the material has the higher thermal conductivity. This would coincide with more binder being present, as more binder will improve the fibre–fibre thermal contact and lower the porosity. This demonstrates how a relatively small material change (probably an increase in the amount of binder) can result in relatively large changes in the through-plane thermal conductivity.

3.2.3. MPL coated PTL stack thermal resistance

Introducing MPL coatings on the PTLs creates a non-uniform structure in the measured samples. As a simplification one can assume that the MPL is attached onto the PTL substrate. In the experiment one can thus consider having two MPLs sandwiched between two PTL substrates. Furthermore, these pairs are placed in the apparatus either alone or in a stack of two or three pairs. Previously, we demonstrated that the PTL–PTL substrate contact resistance is negligible [25], but the MPL–MPL contact resistance is unknown.

The MPL is rather soft and can easily be scraped off the PTL and from this observation one may expect contact resistance to be negligible under the applied pressures. On a meso-level (order of 10 μm) the MPL–MPL and the PTL–PTL interfaces are very different. While the PTL surface side is very rough the MPL surface is very flat and smooth. In stacking the samples as described it was noted that at the highest compaction pressure (only) the PTLs adhered each other while MPL contacts did not. This suggests that the PTLs, when pressed against each other start to form a somewhat integrated sample with contacts similar to contacts in the bulk of the material, which justifies both hypothesis and the observation that PTL–PTL contacts present a negligible contact resistance. Based on the compliance of the MPL layers under study, we also assume in the present work that the MPL–MPL contacts are equally negligible.

Table 5
Comparison of the measured thermal conductivity and the sample thickness as function of ageing time for the different 24 models at 9.3 bar compaction pressure. Thickness is given by μm and thermal conductivity by W K^{-1} m^{-1}. The numbers are reported with double standard deviation.

$Time_{aged}$	0 h	~200 h	~400 h	~600 h	~800 h	~1000 h
$k_{SGL24DA}$	0.33 ± 0.02	0.31 ± 0.02	0.33 ± 0.01	0.32 ± 0.01	0.32 ± 0.01	0.33 ± 0.02
δ	174 ± 5	170 ± 8	173 ± 12	168 ± 3	172 ± 9	175 ± 7
α	137 ± 5	–	129 ± 5	–	–	125 ± 5
$k_{SGL24DC}$	0.345 ± 0.001	0.30 ± 0.03	0.330 ± 0.012	0.38 ± 0.04	0.313 ± 0.019	0.32 ± 0.03
δ	190 ± 2	185 ± 6	192 ± 7	192 ± 6	181 ± 2	186 ± 9
α	143 ± 5[a]	–	141 ± 5[a]	–	–	144 ± 5[a]
$k_{SGL24BC}$	0.369 ± 0.018	0.36 ± 0.06	–	0.38 ± 0.04	0.36 ± 0.06	–
δ	214 ± 7	217 ± 8	–	219 ± 4	220 ± 6	–
α	143 ± 5[a]	–	141 ± 5[a]	–	–	139 ± 5[a]

[a] Measurements done at the MPL surface.

Table 6
Comparison of the measured thermal conductivity and the sample thickness as function of ageing time for the two different PTL models, 24 and 25, at 9.3 bar compaction pressure. Thickness is given by μm and thermal conductivity by W K^{-1} m^{-1}. The numbers are reported with double standard deviation.

$Time_{aged}$	0 h	~200 h	~400 h	~600 h	~800 h	~1000 h
$k_{SGL24BC}$	0.369 ± 0.018	0.36 ± 0.06	–	0.38 ± 0.04	0.36 ± 0.06	–
δ	214 ± 7	217 ± 8	–	219 ± 4	220 ± 6	–
$k_{SGL25BC}$	0.270 ± 0.001	0.31 ± 0.08	0.276 ± 0.001	0.30 ± 0.04	0.26 ± 0.01	0.29 ± 0.06
δ	194 ± 9	187 ± 6	188 ± 3	191 ± 3	191 ± 8	188 ± 7

The relation between the thermal resistance of the stack and the thermal resistance of its sub-components, i.e. R_{PTL-Al}, $R_{PTL/MPL}$ and $R_{MPL-MPL}$, is given by Eq. (4). This model is actually a simplification and can be developed further by accounting for the fact that the MPL intrudes the PTL substrate. To compensate for this, one should subtract for a fraction of the resistance of the PTL $(1 - f_{RPTL})$ that penetrates the MPL, as in Eq. (5). Regardless of how one tries to compensate for this, the outcome is that the PTL substrate, the MPL and the MPL–MPL contact resistance always yields two terms, the contact (R_{PTL-Al}) and the stack. It is clear from these expressions however that the resistance is likely different in different regions of the MPL coated PTL, and that while the overall resistance value will correctly predict the temperature drop over the composite material the temperature gradient within the material will be artificially smoothed by using a single derived value for the thermal conductivity. While the reported thermal conductivities for these materials are convenient for comparing to our previous results and to other published literature, they must be interpreted as effective thermal conductivities.

$$R_{stack} = 2 \cdot R_{PTL-Al} + 2 \cdot N_{pair} \left(R_{PTL/MPL} + \frac{R_{MPL-MPL}}{2} \right) \quad (4)$$

$$R_{stack} = 2 \cdot R_{PTL-Al} + 2 \cdot N_{pair} \left((1 - f_{R_{PTL}}) R_{PTL} + R_{MPL} + \frac{R_{MPL-MPL}}{2} \right) \quad (5)$$

3.3. Water, PTFE and thermal conductivity of PTLs

In this study we have seen that an increased porosity leads to a decreased thermal conductivity of dry PTLs, Section 3.2.2. We have also seen that adding PTFE to the PTL substrate lowers the effective through-plane thermal conductivity of dry PTLs, Section 3.2.1. These two observations are in agreement with reports elsewhere in the literature [25,26,29]. The fact that these properties do not significantly change with ageing, however, is not supported by the NMR and water-PTL contact angle data or the literature – where it is suggested that the PTFE content is lowered [2,5,6] – and therefore we initially expected the thermal conductivity for these (dry) samples should increase with artificial ageing.

Returning to what we found for the water content, contact angle and PTFE-NMR investigation in relation to ageing time, the threshold for water permeability appears to lower slightly along with the ageing time while the thermal conductivity of wet PTLs appears to increase – and in particular for the sample with the most PTFE (SGL 24DA). This suggests that the PTFE, or at least small parts of it, is removed during ageing. Other explanations include oxidation of the carbon surfaces, or fouling of the surface by hydrophilic contaminants, though the NMR study supports the lowered PTFE content. Moreover, we argue that the PTFE is primarily removed from the open areas away from the carbon fibre to fibre connection regions and perhaps very small regions near the fibre contacts such that the amount is detectable by NMR when comparing pristine material and material aged for 1000 h. PTFE removed from the fibre surfaces away from the contacts would not be expected to change the thermal conductivity to any significant degree but it would definitely have an impact on the contact angle as measured by sessile drop and the NMR measurements. These changes result in more water entering the PTL and the possibility to bridge fibres, effectively increasing the fibre to fibre contact area and increasing the overall thermal conductivity. Thus the preferential removal of PTFE away from the points of fibre contact can explain the relatively unchanging dry thermal conductivity and simultaneously the increase in wet thermal conductivity.

Fig. 7 illustrates our mechanistic explanation, where we depict the fibre to fibre connection for two fibres, two fibres with PTFE in the junction region and one with reduced PTFE away from the contact point of the fibre to fibre intersection (i.e. the PTFE remains in

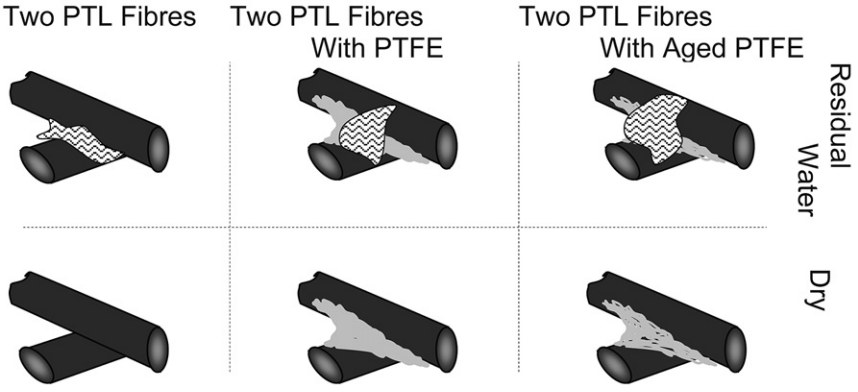

Fig. 7. A visual comparison of a possible contact between two carbon fibres without binder or PTFE (left) with PTFE binder (centre) and aged PTFE (right) with (upper series) and without (lower series) residual water.

between.). Also this figure suggests how more water, either (as illustrated) by larger local presence or otherwise (not illustrated) by more frequent presence, enhances the thermal energy transport region.

4. Conclusion

In the present study it was found that heating PTLs (Porous Transport Layer) containing PTFE (Teflon) for up to 1000 h in air bubbled water does not significantly change the through-plane thermal conductivity for dry PTLs.

This ageing procedure does however result in lower contact angles (became less hydrophobic) as measured by sessile drops and the PTFE content was found to decrease. In response, the thermal conductivity of PTLs containing water increased with ageing time.

It is our understanding that, since the PTL became more susceptible to water and the thermal conductivity of the dry materials did not change, the PTFE remained in the carbon fibre to fibre contact regions during the applied ageing procedure and that PTFE was removed elsewhere in the PTL.

Measuring the thermal conductivity of several different dry PTLs coated with MPL (Micro Porous Layers) we also observed that the PTFE content in the substrate is of greater importance for the material average thermal conductivity than the addition of a MPL.

Acknowledgement

The Norwegian Research Council is acknowledged for financial support, FRIENERGI, grant number 197598 and the RENERGI, grant number 164466/S30.

The Fuel Cell Technologies Program at the U.S. Department of Energy EERE is also acknowledged for financial support, with particular acknowledgement to Technology Development Manager Nancy Garland. Contact angle tests were performed by Chris Rulison at Augustine Scientific (Newbury, OH).

Appendix A. An example of a measurement

Measuring SGL DA by stacking 1, 3 and 5 discs in the apparatus is presented in Fig. A.8. Also indicated is the regression using micrometre. Converting the regression coefficient one gets the reported thermal conductivity of 0.332 ± 0.018 W K^{-1} m^{-1}.

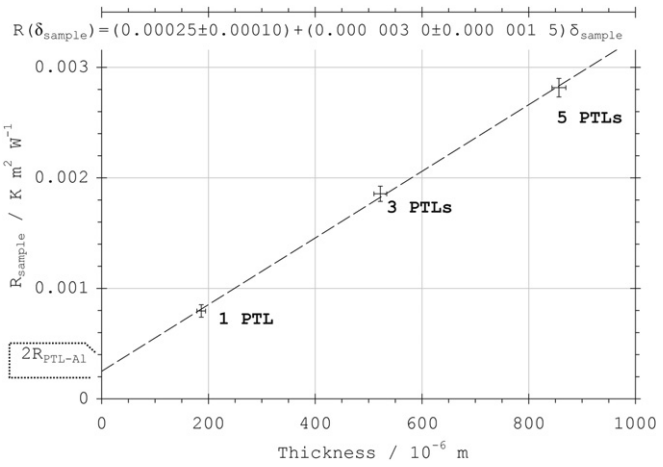

Fig. A.8. Measured resistance and thickness for different stacks of SGL 24DA. Also presented is the linear regression – using thickness in micrometre.

Appendix B. Tabulated raw data

In this Appendix we give a broader range of some of the data. The chosen data sets are for the dry and the wet measurements using SGL 24DA.

Table B.7. Measured thickness, thermal conductivity and double contact resistivity of SGL 24DA with and without water at different compaction pressures, ~295 K and different artificial ageing time. Reported errors are double standard deviations.

	Dry Samples			Wet Samples			
P/bar	$\delta_{0h}/10^{-6}$m	k_{0h}/W K^{-1} m^{-2}	$2{\cdot}R_{0h}^{Al-PTL}/10^{-4}$ K m^2 W^{-1}	$\delta_{0h}/10^{-6}$ m	k_{0h}/W K^{-1} m^{-2}	$2{\cdot}R_{0h}^{Al-PTL}/10^{-4}$ K m^2 W^{-1}	S %
4.6	190 ± 18	0.247 ± 0.001	4.6 ± 0.1	112 ± 71	0.42 ± 0.14	5 ± 4	25±15
9.3	177 ± 16	0.332 ± 0.018	2.5 ± 1.0	106 ± 63	0.50 ± 0.14	3 ± 3	28±16
13.9	166 ± 15	0.403 ± 0.017	1.7 ± 0.7	99 ± 59	0.57 ± 0.12	2 ± 2	30±17
P/bar	$\delta_{210h}/10^{-6}$ m	k_{210h}/W K^{-1} m^{-2}	$2{\cdot}R_{210h}^{Al-PTL}/10^{-4}$ K m^2 W^{-1}	$\delta_{210h}/10^{-6}$ m	k_{210h}/W K^{-1} m^{-2}	$2{\cdot}R_{210h}^{Al-PTL}/10^{-4}$ K m^2 W^{-1}	S %
4.6	188 ± 16	0.23 ± 0.02	3.4 ± 1.5	112 ± 70	0.51 ± 0.08	4.2 ± 1.9	30 ± 22
9.3	173 ± 16	0.31 ± 0.02	1.9 ± 1.0	104 ± 62	0.58 ± 0.02	1.9 ± 0.3	34 ± 25
13.9	160 ± 15	0.38 ± 0.03	1.5 ± 1.0	96 ± 58	0.69 ± 0.09	1.9 ± 0.9	37 ± 27
P/bar	$\delta_{412h}/10^{-6}$ m	k_{412h}/W K^{-1} m^{-2}	$2{\cdot}R_{412h}^{Al-PTL}/10^{-4}$ K m^2 W^{-1}	$\delta_{412h}/10^{-6}$ m	k_{412h}/W K^{-1} m^{-2}	$2{\cdot}R_{412h}^{Al-PTL}/10^{-4}$ K m^2 W^{-1}	S %
4.6	185 ± 11	0.241 ± 0.019	3.0 ± 2.1	130 ± 56	0.82 ± 0.15	8.4 ± 1.4	32 ± 21
9.3	174 ± 12	0.331 ± 0.013	2.1 ± 0.7	119 ± 52	0.85 ± 0.25	5 ± 2	35 ± 23
13.9	162 ± 15	0.397 ± 0.006	1.4 ± 0.2	111 ± 48	±	±	39 ± 26
P/bar	$\delta_{600h}/10^{-6}$ m	k_{600h}/W K^{-1} m^{-2}	$2{\cdot}R_{600h}^{Al-PTL}/10^{-4}$ K m^2 W^{-1}	$\delta_{600h}/10^{-6}$ m	k_{600h}/W K^{-1} m^{-2}	$2{\cdot}R_{600h}^{Al-PTL}/10^{-4}$ K m^2 W^{-1}	S %
4.6	190 ± 19	0.246 ± 0.003	4.0 ± 0.3	110 ± 72	0.47 ± 0.26	3 ± 7	33 ± 26
9.3	175 ± 16	0.319 ± 0.006	2.0 ± 0.3	103 ± 63	0.58 ± 0.27	2 ± 4	37 ± 28
13.9	162 ± 15	0.382 ± 0.014	1.2 ± 0.5	96 ± 58	0.65 ± 0.29	1 ± 3	41 ± 31
P/bar	$\delta_{793h}/10^{-6}$ m	k_{793h}/W K^{-1} m^{-2}	$2{\cdot}R_{793h}^{Al-PTL}/10^{-4}$ K m^2 W^{-1}	$\delta_{793h}/10^{-6}$ m	k_{793h}/W K^{-1} m^{-2}	$2{\cdot}R_{793h}^{Al-PTL}/10^{-4}$ K m^2 W^{-1}	S %
4.6	185 ± 6	0.25 ± 0.03	4.9 ± 2.7	113 ± 68	0.81 ± 0.04	10.0 ± 0.3	30 ± 17
9.3	170 ± 5	0.320 ± 0.004	2.2 ± 0.2	105 ± 60	0.94 ± 0.04	6.8 ± 0.2	34 ± 18
13.9	158 ± 6	0.390 ± 0.003	1.5 ± 0.1	96 ± 55	0.95 ± 0.04	4.8 ± 0.2	37 ± 20
P/bar	$\delta_{1001h}/10^{-6}$ m	k_{1001h}/W K^{-1} m^{-2}	$2{\cdot}R_{1001h}^{Al-PTL}/10^{-4}$ K m^2 W^{-1}	$\delta_{1001h}/10^{-6}$ m	k_{1001h}/W K^{-1} m^{-2}	$2{\cdot}R_{1001h}^{Al-PTL}/10^{-4}$ K m^2 W^{-1}	S %
4.6	180 ± 5	0.25 ± 0.02	3.8 ± 1.5	93 ± 1	0.74 ± 0.78	4 ± 6	41 ± 17
9.3	167 ± 6	0.33 ± 0.02	2.6 ± 1.3	88 ± 4	0.88 ± 0.72	3 ± 3	44 ± 20
13.9	156 ± 7	0.39 ± 0.02	1.7 ± 0.8	83 ± 4	0.96 ± 0.81	2 ± 3	47 ± 21

References

[1] F. de Bruijn, V.A.T. Dam, G. Janssen, Fuel Cells 8 (2008) 1–22.
[2] X. Yuan, H. Li, S. Zhang, J. Martin, H. Wang, J. Power Sources 196 (2011) 9107–9116.
[3] S. Cleghorn, D. Mayfield, D. Moore, G. Rusch, T. Sherman, N. Sisifo, U. Beuscher, J. Power Sources 158 (2006) 446–454.
[4] C. Lee, W. Merida, J. Power Sources 164 (2007) 141–153.
[5] M. Schulze, N. Wagner, T. Kaz, K. Friedrich, Electrochim. Acta 52 (2007) 2328–2336.
[6] R. Kumar, V. Radhakrishnan, P. Haridoss, Int. J. Hydrogen Energy 36 (2011) 7207–7211.
[7] S. Kjelstrup, A. Røsgjorde, J. Phys. Rev. B 109 (2005) 9020.
[8] O. Burheim, P.J.S. Vie, S. Møller-Holst, J. Pharoah, S. Kjelstrup, Electrochim. Acta 55 (2010) 935–942.
[9] O. Burheim, Signe Kjelstrup, J.G. Pharoah, P.J.S. Vie, S. Møller-Holst, Electrochim. Acta 56 (2011) 3248–3257.
[10] K. Kinoshita, Electrochemical Oxygen Technology, Interscience, New York, 1992.
[11] P. Vie, S. Kjelstrup, Electrochim. Acta 49 (2004) 1069–1077.
[12] J. Pharoah, O. Burheim, J. Power Sources 195 (2010) 5235–5245.
[13] P. Reucroft, D. Rivin, N. Schneider, Polymer 43 (2002) 5157–5161.
[14] C. Bapat, S. Thynell, J. Heat Transf. 129 (2007) 1109–1118.
[15] A. Weber, J. Newman, Chem. Rev. 104.
[16] G. Alberti, M. Casciola, L. Massinelli, B. Bauer, J. Membr. Sci. 185 (2001) 73–81.
[17] F. Bauer, S. Denneler, M. Willert-Porada, J. Polym. Sci. B 43 (2005) 786–795.
[18] S. Kim, M. Mench, J. Electrochem. Soc. 156 (2009) B353–B362.
[19] J. Pharoah, K. Karan, W. Sun, J. Power Sources 161 (2006) 214–224.
[20] F. Danes, J. Bardon, 36 (2008) 200–208.
[21] E. Sadeghi, M. Bahrami, N. Djilali, J. Power Sources 179 (2008) 200–208.
[22] E. Sadeghi, N. Djilali, M. Bahrami, J. Power Sources 196 (2011) 3565–3571.
[23] P. Teertstra, G. Karimi, X. Li, Electrochim. Acta (in press).
[24] N. Zamel, E. Litovsky, S. Shakhshir, X. Li, J. Kleiman, Appl. Energy 88 (2011) 3042–3050.
[25] O. Burheim, P. Vie, J. Pharoah, S. Kjelstrup, J. Power Sources 195 (2010) 249–256.
[26] O. Burheim, H. Lampert, J. Pharoah, P. Vie, S. Kjelstrup, ASME J. Fuel Cell. Sci. Technol. 8 (April 2011). 021013–1–11.
[27] J. Ramousse, O. Lottin, S. Didierjean, D. Maillet, Int. J. Therm. Sci. 47 (2008) 1–6.
[28] J. Ihonen, M. Mikkola, G. Lindhberg, J. Electrochem. Soc. 151 (2004) A1152–A1161.
[29] M. Khandelwal, M. Mench, J. Power Sources 161 (2006) 1106–1115.
[30] J. Ramousse, O. Lottin, S. Didierjean, D. Maillet, J. Power Sources 192 (2009) 435–441.
[31] N. Zamel, E. Litovsky, S. Shakhshir, X. Li, J. Kleiman, Int. J. Hydrogen Energy 36 (2011) 12618–12625.
[32] E. Sadeghi, N. Djilali, M. Bahrami, J. Power Sources 196 (2011) 246–254.
[33] E. Sadeghi, N. Djilali, M. Bahrami, J. Power Sources 195 (2010) 8104–8109.
[34] R. Borup, J. Meyers, B. Pivovar, Y.S. Kim, R. Mukundan, N. Garland, D. Myers, M. Wilson, F. Garzon, D. Wood, P. Zelenay, K. More, K. Stroh, T. Zawodzinski, J. Boncella, J.E. McGrath, M. Inaba, K. Miyatake, M. Hori, K. Ota, Z. Ogumi, S. Miyata, A. Nishikata, Z. Siroma, Y. Uchimoto, K. Yasuda, K. Kimijima, N. Iwashita, Chem. Rev. 107 (10) (2007) 3904–3951.